* **Manuscript**

Accepted for publication in Ocean Engineering, 2008

Removing irregular frequencies by a partial discontinuous higher order boundary element method

L. Sun, B. Teng*, C. F. Liu

State Key Laboratory of Coastal and Offshore Engineering, Dalian University of Technology, Dalian 116024, PR China

Abstract

The phenomenon of irregular frequencies is a puzzle in the course of calculating the interaction of waves and structures by the boundary element method. To remove the irregular frequencies, the modified integral domain method is adopted, and continuous higher order elements and partial discontinuous higher order elements are used for discretization. By these means, the effects of the irregular frequencies are effectively removed. Effective strategies have been adopted to deal with singular integrals and nearly singular integrals at different situations. The numerical results of the horizontal wave force on a uniform cylinder in the first order and second order diffraction problems show that the present method has a good validity. At the same time, the influence of collocation parameter on accuracy of numerical results is examined in detail.

Key words: Irregular frequency; Partial discontinuous higher order element; Boundary integral equation

1. Introduction

With the exploitation of ocean resources, various kinds of ships and maritime structures have come forth. The security of them under wave effect is a critical point in practical projects. There are mainly four kinds of research methods for the problems, including experimental method, analytic method, semi-analytic method and numerical method. However, experimental method needs a great quantity of investment, while analytic method and semi-analytic method can only be applied to structures with simple

* Corresponding author. Tel.: +86-411-84707103; Fax: +86-411-84708526.
E-mail address: bteng@dlut.edu.cn (B. Teng).

geometries. Therefore, the analyses of complex structures are usually accomplished by numerical methods. Boundary element method is often adopted to analyze the problems on the interaction of waves and structures because it usually needs less computation efforts and is easier meshed than domain methods.

However, the phenomenon of irregular frequencies arises in the computation for surface-piercing bodies by ordinary boundary element method, which usually uses the Green function satisfying the first order free surface condition to save CPU time and storage. The irregular frequencies make the numerical computation embarrassed. For bodies with simple geometries, the positions of irregular frequencies can be determined by theoretical analysis. While for complex structures, it can hardly distinguish whether the results have been polluted by irregular frequencies. This is more serious for higher order problems, because correct results can only be achieved on the condition that the computations at the same order and the lower orders are all free of irregular frequencies.

Different methods have been adopted to eliminate the irregular frequencies. For two dimensional problems, Ogilvie and Shin (1978) placed a point wave source on the interior free surface to remove the first irregular frequency; Ursell (1981) showed that a series of singularities must be used to remove more irregular frequencies; Ohmatsu (1983) used a combined integral equation method for radiation problem in infinite water depth; Duan and He (2002) adopted mixed source and dipole distribution model in the integral equation. For three dimensional problems, Lee and Sclavounos (1989) superposed the classical integral equation and its normal derivative with respect to the field point, multiplying the latter by a complex coupling constant. In the derived integral equation, the second derivative of Green's function is used, which has a singular kernel of $1/r^3$ when field points are very close to source points. (The integration of this singularity is very difficult to compute in higher order boundary element method for three dimensional problems.) All the methods mentioned above are implemented by the constant panel method. To remove the irregular frequencies from higher order boundary element method, Teng and Li (1996) used the modified integral domain method by adding an artificial 'lid' on the inner water plane. To overcome the conflict that the velocity potential on the 'lid' should be zero, and yet the potential on the body surface should not be zero, they only added the 'lid' on a subdomain of the inner water plane which does not touch the body surface. Examinations show that this strategy can move the irregular frequencies to higher frequency, rather than removing the irregular frequencies totally, and how high the irregular frequencies will be pushed to depending on the size of the 'lid'.

In the present research, Teng and Li's (1996) modified integral equation method is adopted and a whole 'lid' is put on the inner water plane. To overcome the conflict of velocity potentials at the inner water line (the intersection curve of the body surface and the 'lid'), partial discontinuous higher order boundary elements are used to discretize the physical quality around the rim of the 'lid'. By this means, discontinuity of physical quality at the rim of the 'lid' is resolved successfully. Validation of numerical examples indicated that the present method can remove the irregular frequencies completely in three dimensional water wave problems.

2. Integral equations and irregular frequencies

Under the assumptions of an incompressible and inviscid fluid with irrotational motion, there exists a scalar velocity potential $\Phi(x, y, z, t)$ which satisfies the Laplace equation in the fluid domain Ω (see Fig. 1), i.e.

$$\nabla^2 \Phi(x, y, z, t) = 0 \tag{1}$$

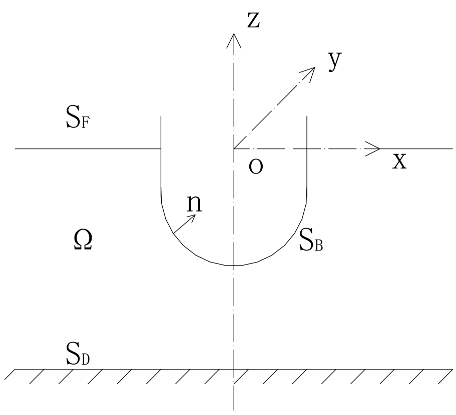

Fig.1 Definition of coordinates system

When the waves are weakly nonlinear, the solution of $\Phi(x, y, z, t)$ can be assumed to take the form of power series with respect to a perturbation parameter ε ($\varepsilon = kA \ll 1$, k is wave number, and A is wave amplitude), which is the order of wave steepness.

$$\Phi = \varepsilon \Phi^{(1)} + \varepsilon^2 \Phi^{(2)} + \cdots \tag{2}$$

For monochromatic incident waves, the first order and second order velocity potential can be expressed in complex spatial forms as:

$$\Phi^{(1)}(x,y,z,t) = \mathrm{Re}[\varphi^{(1)}(x,y,z)e^{-i\omega t}] \tag{3.a}$$

$$\Phi^{(2)}(x,y,z,t) = \mathrm{Re}[\varphi^{(2)}(x,y,z)e^{-2i\omega t}] + \overline{\Phi}^{(2)}(x,y,z) \tag{3.b}$$

Note that the contribution of the steady part of second order potential in (3.b) to the pressure (hence force) or free surface is at most $O(\varepsilon^3)$, which is out of present research. The complex potential $\varphi^{(j)}$ (j=1, 2) also satisfies the Laplace equation. For the convenience in numerical calculation, it can be further decomposed into an incident potential $\varphi_i^{(j)}$ and a diffraction potential $\varphi_d^{(j)}$ for the diffraction problem at each order.

In addition, the diffraction potential $\varphi_d^{(j)}$ must satisfy the following boundary conditions:

The free surface boundary condition on S_F:

$$\frac{\partial \varphi_d^{(j)}}{\partial z} - v^{(j)}\varphi_d^{(j)} = q^{(j)} \tag{4}$$

in which, $v^{(1)} = \frac{\omega^2}{g}$, $v^{(2)} = \frac{4\omega^2}{g}$, and the forcing term at each order (Chau, 1989)

$$q^{(1)} = 0 \tag{5.a}$$

$$\begin{aligned} q^{(2)} = &-\frac{i\omega}{2g}\phi_i^{(1)}\left[-\frac{\omega^2}{g}\frac{\partial \phi_d^{(1)}}{\partial z} + \frac{\partial^2 \phi_d^{(1)}}{\partial z^2}\right] - \frac{i\omega}{2g}\phi_d^{(1)}\left[-\frac{\omega^2}{g}\frac{\partial \phi_i^{(1)}}{\partial z} + \frac{\partial^2 \phi_i^{(1)}}{\partial z^2}\right] \\ &-\frac{i\omega}{2g}\phi_d^{(1)}\left[-\frac{\omega^2}{g}\frac{\partial \phi_d^{(1)}}{\partial z} + \frac{\partial^2 \phi_d^{(1)}}{\partial z^2}\right] + \frac{i\omega}{g}\left[\left(\frac{\partial \phi_d^{(1)}}{\partial x}\right)^2 + \left(\frac{\partial \phi_d^{(1)}}{\partial y}\right)^2 + \left(\frac{\partial \phi_d^{(1)}}{\partial z}\right)^2\right] \\ &+\frac{2i\omega}{g}\left[\left(\frac{\partial \phi_i^{(1)}}{\partial x}\right)\left(\frac{\partial \phi_d^{(1)}}{\partial x}\right) + \left(\frac{\partial \phi_i^{(1)}}{\partial y}\right)\left(\frac{\partial \phi_d^{(1)}}{\partial y}\right) + \left(\frac{\partial \phi_i^{(1)}}{\partial z}\right)\left(\frac{\partial \phi_d^{(1)}}{\partial z}\right)\right] \end{aligned} \tag{5.b}$$

The sea bed condition on S_D:

$$\frac{\partial \varphi_d^{(j)}}{\partial z} = 0 \tag{6}$$

The rigid impermeable body surface condition on S_B:

$$\frac{\partial \varphi_d^{(j)}}{\partial n} = -\frac{\partial \varphi_i^{(j)}}{\partial n} \tag{7}$$

The radiation condition at infinity for the first order problem:

$$\lim_{r\to\infty}\sqrt{r}\left(\frac{\partial \varphi_d^{(1)}}{\partial r} - \mathrm{i}k\varphi_d^{(1)}\right) = 0 \tag{8.a}$$

The weak radiation condition at infinity for the second order problem (Molin, 1979):

$$\phi_d^{(2)} \simeq \frac{1}{\sqrt{r}}\left[L_1(\theta,z)e^{ikr} + L_2(\theta,z)e^{ikr(1+\cos\theta)}\right] \tag{8.b}$$

where L_1 and L_2 are independent of r.

Applying the classical Green second identity and using the Green's function (John, 1950) which satisfies the first order wave conditions, we can get the following integral equation:

$$\alpha\varphi_d^{(j)}(\vec{x}_0) - \iint_{S_B} \varphi_d^{(j)}(\vec{x})\frac{\partial G^{(j)}(\vec{x},\vec{x}_0)}{\partial n}ds = \iint_{S_B} G^{(j)}(\vec{x},\vec{x}_0)\frac{\partial \varphi_i^{(j)}(\vec{x})}{\partial n}ds - \iint_{S_F} q^{(j)}(\vec{x})G^{(j)}(\vec{x},\vec{x}_0)ds \tag{9}$$

where α is the solid angle coefficient. The Green's functions for the first order and second order problems are

$$G^{(j)}(\vec{x},\vec{x}_0) = -\frac{1}{4\pi}\left[\frac{1}{r} + \frac{1}{r_2} + 2\int_0^\infty \frac{(\mu+\nu^{(j)})e^{-\mu d}\cosh[\mu(z_0+d)]\cosh[\mu(z+d)]}{\mu\sinh(\mu d) - \nu^{(j)}\cosh(\mu d)}J_0(\mu R)d\mu\right] \tag{10}$$

in which $\vec{x} = (x,y,z)$ are the coordinates of the field point, $\vec{x}_0 = (x_0, y_0, z_0)$ are the coordinates of the source point and d is the water depth, $R = \sqrt{(x-x_0)^2 + (y-y_0)^2}$, $r = \sqrt{R^2 + (z-z_0)^2}$, $r_2 = \sqrt{R^2 + (z+2d+z_0)^2}$.

To removing the solid angle coefficient α, an integral equation obtained inside the body is supplemented to the integral equation (9), and it yields a new integral equation (Teng and Eatock Taylor, 1995)

$$\begin{aligned}\varphi_d^{(j)}(\vec{x}_0) + \iint_{S_B}\left[\varphi_d^{(j)}(\vec{x}_0)\frac{\partial G_0(\vec{x},\vec{x}_0)}{\partial n} - \varphi_d^{(j)}(\vec{x})\frac{\partial G^{(j)}(\vec{x},\vec{x}_0)}{\partial n}\right]ds \\ = \iint_{S_B} G^{(j)}(\vec{x},\vec{x}_0)\frac{\partial \varphi_i^{(j)}(\vec{x})}{\partial n}ds - \iint_{S_F} q^{(j)}(\vec{x})G^{(j)}(\vec{x},\vec{x}_0)ds\end{aligned} \tag{11}$$

where $G_0(\vec{x},\vec{x}_0)$ satisfies the rigid impermeable water surface condition ($\frac{\partial G_0}{\partial z} = 0$) and the seabed condition.

A set of linear equations are obtained after discretizing the integral equation (11). Diffraction potential on the body surface can be resolved from the set of linear equations. Then the first order and second order wave forces are obtained by integration of wave pressure over the body surface. The first order wave force can be written into

$$F^{(1)} = \mathrm{Re}[f^{(1)} e^{-i\omega t}] \tag{12}$$

in which,

$$f^{(1)} = i\omega\rho \iint_{S_B} \phi^{(1)} \bullet \vec{n} ds \tag{13}$$

and the second order wave force can be expressed as

$$F^{(2)} = \mathrm{Re}[f^{(2)} e^{-2i\omega t}] + f_m^{(2)} \tag{14}$$

in which

$$f^{(2)} = \iint_{S_B} 2i\omega\rho\phi^{(2)} \bullet \vec{n} ds - \iint_{S_B} \frac{\rho}{4} \nabla\phi^{(1)} \bullet \nabla\phi^{(1)} \bullet \vec{n} ds - \frac{\rho\omega^2}{4g} \int_{water\ line} \phi^{(1)^2} \bullet \vec{n} dl \tag{15}$$

and $f_m^{(2)}$ represents second order mean drift force. Our study puts emphasis on the first order wave force and second order wave force due to the second order potential. The process of solving the first and second order problems is illustrated in the following flow chart.

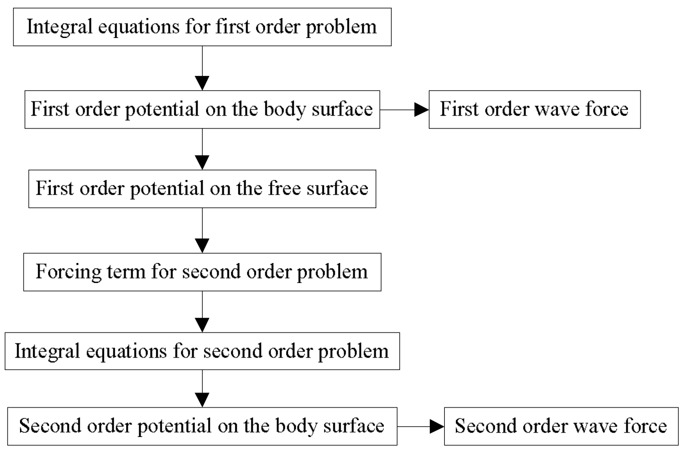

Fig.2 Flow chart of computation

Lamb (1932) has proved that the solution of following integral equation

$$\alpha U(\vec{x}_0) - \iint_{S_B} U(\vec{x}) \frac{\partial G(\vec{x}, \vec{x}_0)}{\partial n} ds = 0 \tag{16}$$

is not unique at certain frequencies. Therefore, the solution of integral equation (9) is not unique at those frequencies and neither of integral equation (11). This phenomenon is called as the irregular frequencies phenomenon, and the corresponding frequencies are named as irregular frequencies. Further introduction can be found in the book of Mei (1989).

3. Modified integral equations

Teng and Li (1996) tried to remove irregular frequencies by modifying the integral domain. The integral domain (see Fig.3) in their method includes body surface S_B and a subdomain of the inner water plane S_{WP}.

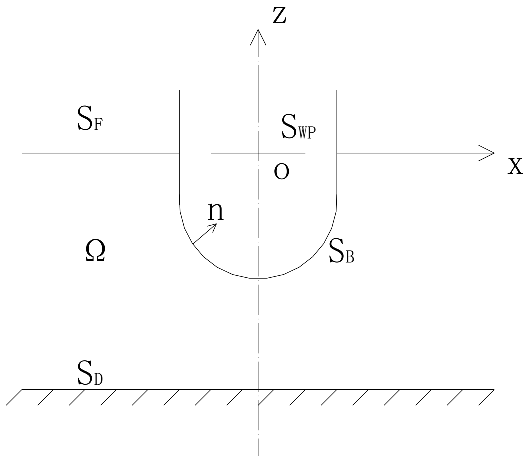

Fig.3 Domain of integration

They discretized the body surface into N higher order elements with n nodes and the inner water plane into M elements with m nodes. To remove the irregular frequencies, the source point $\vec{x}_0$ is allocated at all n nodes on the body surface S_B and all m nodes on the inner water plane S_{WP}. Then a set of overdeterminated linear equations can be obtained

$$\left[A_1^{(j)}\right]_{(n+m)\times n}\left\{\varphi_d^{(j)}\right\}_n=\left\{B^{(j)}\right\}_{(n+m)} \tag{17}$$

The above linear equations will give a set of unique solutions, but have the awkward of overdetermination. To avoid the overdetermination, the following integral equations with zero solution have been introduced

$$\begin{cases} \psi(\vec{x}_0) + \iint_{S_{WP}} \psi(\vec{x}) \dfrac{\partial G^{(j)}(\vec{x},\vec{x}_0)}{\partial n} ds = 0 & (\vec{x}_0 \in S_{WP}) \\ -\iint_{S_{WP}} \psi(\vec{x}) \dfrac{\partial G^{(j)}(\vec{x},\vec{x}_0)}{\partial n} ds = 0 & (\vec{x}_0 \in S_B) \end{cases} \tag{18}$$

After discretization, another linear system can be obtained

$$\left[A_2^{(j)}\right]_{(n+m)\times m} \left\{\psi^{(j)}\right\}_m = \left\{0\right\}_{(n+m)} \tag{19}$$

Combining Eq. (17) with Eq. (19), we can develop a new set of equations

$$\left[A^{(j)}\right]_{(n+m)\times(n+m)} \begin{Bmatrix} \varphi_d{}^{(j)} \\ \psi^{(j)} \end{Bmatrix}_{(n+m)} = \left\{B^{(j)}\right\}_{(n+m)} \tag{20}$$

This set of equations is not overdetermined, so it can be solved directly.

The value of velocity potential on the inner water plane must be zero, and yet that on the body surface should have a certain value. Due to the continuous higher order boundary elements can not deal with the discontinuity of velocity potential at the common boundary of the inner water plane and body surface, they only extended the auxiliary integral domain to a portion of the inner water plane. Extensive numerical examinations show that this strategy can not remove the irregular frequencies ultimately, but move the irregular frequencies to higher position.

To remove the irregular frequencies totally, the full ‘lid’ is used in the present method. Partial discontinuous boundary elements are adopted to overcome the discontinuity of velocity potentials at the inner water line (the intersection curve of the body surface and the ‘lid’).

4. Partial discontinuous boundary element method

On the basis of foregoing analyses, continuous higher order boundary elements and partial discontinuous higher order boundary elements are used to discretized the integral equations which Teng and Li (1996) adopted. For all of geometric qualities, continuous higher order boundary elements are adopted to express the surface of integration domain. For the physical qualities on the body surface and interior part of the inner water plane, continuous higher order boundary elements are adopted; for the physical qualities on the boundary of the inner water plane, partial discontinuous higher order boundary elements are adopted. By this means, not only the geometric continuity is ensured, but also the physical discontinuity on the interface of body surface and the inner water plane is satisfied.

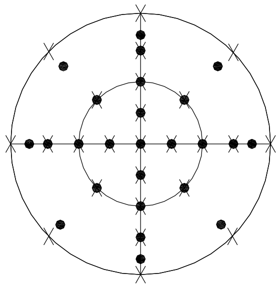

Fig.4 Sketch of elements on the inner water plane

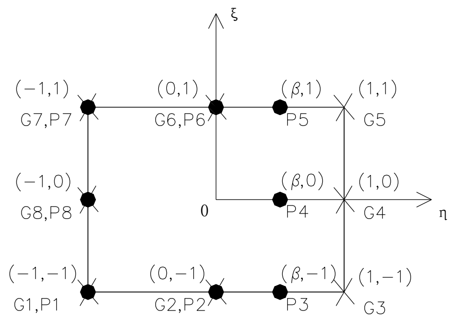

Fig.5 Distribution of nodes in quadrilateral element under the local coordinate system

On the inner water plane, the distribution of elements is shown as Fig.4 (× represents geometric nodes; ● represents physical nodes), and the distribution of nodes in partial discontinuous element in the local coordinate system is shown as Fig.5 (0< β <1). In Fig.5, G1, G2, G3, G4, G5, G6, G7, G8 are geometric nodes; P1, P2, P3, P4, P5, P6, P7, P8 are physical nodes.

Interpolation functions for continuous higher order boundary elements are used to describe the variation of geometric qualities and physical qualities which change continuously, i.e.

$$x = \sum_{i=1}^{8} n_i x_i \,,\; y = \sum_{i=1}^{8} n_i y_i \,,\; z = \sum_{i=1}^{8} n_i z_i \,,\; u = \sum_{i=1}^{8} n_i u_i \tag{21}$$

in which,

$$n_1 = -\frac{(1-\xi)(1-\eta)(1+\xi+\eta)}{4} \qquad n_2 = \frac{(1-\xi^2)(1-\eta)}{2}$$

$$n_3 = \frac{(1+\xi)(1-\eta)(\xi-\eta-1)}{4} \qquad n_4 = \frac{(1-\eta^2)(1+\xi)}{2}$$

$$n_5 = \frac{(1+\xi)(1+\eta)(\xi+\eta-1)}{4} \qquad n_6 = \frac{(1-\xi^2)(1+\eta)}{2}$$

$$n_7 = -\frac{(1-\xi)(1+\eta)(\xi-\eta+1)}{4} \qquad n_8 = \frac{(1-\eta^2)(1-\xi)}{2} \tag{22}$$

However, interpolation functions for partial discontinuous higher order boundary elements are used to describe the variation of physical qualities at boundary where the values of physical qualities are discontinuous, i.e.

$$u = \sum_{i=1}^{8} h_i u_i \tag{23}$$

where,

$$h_1 = \frac{(\eta - 1)(\eta + \xi + 1)(\beta - \xi)}{2(\beta + 1)} \qquad h_2 = \frac{(1-\eta)(1+\xi)(\beta - \xi)}{2\beta}$$

$$h_3 = \frac{(\eta - 1)(1 + \xi)(\eta\beta - \xi + \beta)}{2\beta(\beta + 1)} \qquad h_4 = \frac{(1+\xi)(1-\eta^2)}{\beta + 1}$$

$$h_5 = \frac{(\eta + 1)(\xi + 1)(\xi + \beta\eta - \beta)}{2\beta(\beta + 1)} \qquad h_6 = \frac{(\eta + 1)(\xi + 1)(\beta - \xi)}{2\beta}$$

$$h_7 = \frac{(\eta + 1)(\xi - \eta + 1)(\xi - \beta)}{2(\beta + 1)} \qquad h_8 = \frac{(\eta^2 - 1)(\xi - \beta)}{\beta + 1} \tag{24}$$

5. Computation of infinite integral on the free surface for second order problem

In integral equation (9) and (11), infinite integral on the free surface is difficult to evaluate in second order problem because the corresponding integrand is highly oscillatory and decays slowly at infinity. Special attention should be paid to evaluation of this component by fast and accurate algorithms. Effective methods of accelerating its convergence for arbitrary bodies were demonstrated by Chau and Eatock Taylor (1988). The method described in detail by Chau (1989) is adopted in present research.

Another problem that should be taken into consideration is calculation of the first order diffraction potential on the free surface, which is obtained by the following equation.

$$\varphi_d^{(1)}(\vec{x}_0) = \iint_{S_B} \varphi_d^{(1)}(\vec{x}) \frac{\partial G^{(1)}(\vec{x}, \vec{x}_0)}{\partial n} ds + \iint_{S_B} G^{(1)}(\vec{x}, \vec{x}_0) \frac{\partial \varphi_i^{(1)}(\vec{x})}{\partial n} ds \tag{25}$$

where $\vec{x}_0 = (x_0, y_0, z_0)$ is the coordinates of computing point on the free surface and $\vec{x} = (x, y, z)$ is the coordinates of integrating point on the body surface. There will arise the first order and second order nearly singularity when the required points are near to the body surface. Accurate results can not be obtained by direct integration in such situation. There are mainly two kinds of methods to deal with nearly singular behaviors: analytical method and numerical method. Analytical method usually cancel the nearly singularities by making some transformation to the integral equations (Teng, 1999). For numerical method, Chau (1989) gave some suggestion in his thesis. In present research, the self-adaptive integration scheme proposed by Sun (to be published) is adopted, which can get accurate integral results.

6. Strategies to other singular and nearly singular integrals

There is a large amount of integration in the computation. The accuracy of the integration has important effect on the numerical results. Besides the nearly singular integrals mentioned above, there are other singular and nearly singular integrals in calculation. Careful consideration should be given to these singular and nearly singular integrals.

6.1 First order singular integrals

When the source point is in the integration element, the integral $\iint_{S_B} G^{(j)}(\vec{x},\vec{x}_0)\frac{\partial \varphi_i^{(j)}(\vec{x},\vec{x}_0)}{\partial n}ds$ has first order singularity. To avoid appreciable errors induced by evaluating this integral directly, triangular polar coordinate transformation proposed by Li et al. (1985) is adopted in this paper.

6.2 First order nearly singular integrals

When the collocation parameter β of discontinuous boundary element approaches to 1.0, some source points on the inner water plane would be very close to the integration element on the body surface, and the integral $\iint_{S_B} G^{(j)}(\vec{x},\vec{x}_0)\frac{\partial \varphi_i^{(j)}(\vec{x},\vec{x}_0)}{\partial n}ds$ has first order nearly singularity. Similarly, a triangular polar coordinate transformation is adopted here to increase accuracy of integration. When the minimal distance between the source point and field points is less than the specified criterion, the original element is subdivided into four or six triangular sub-elements for different situation (see Fig.6, ● presents the field point nearest to the source point). The following process is the same to the corresponding procedure for the first order singular integrals. In present research, criterion is selected as $EL=\frac{1}{4}\sum_{i=1}^{8}EL_i$ (EL_i is the distance between two adjacent field points). After transformation, integration points would concentrate to the source point (see Fig.7, in which ● is the field point nearest to the source point), and the improvement of the accuracy is mainly due to the lumping effect.

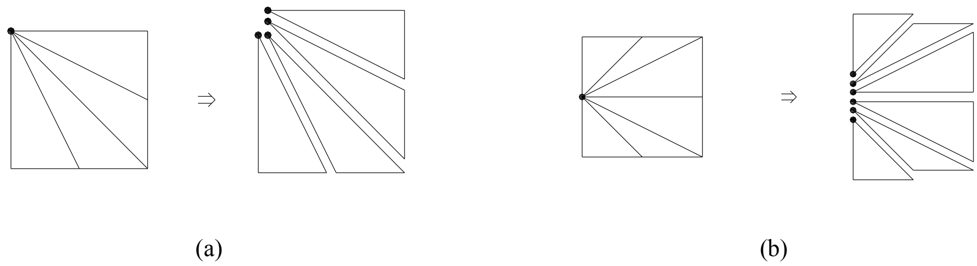

Fig.6 Divided into triangular sub-elements

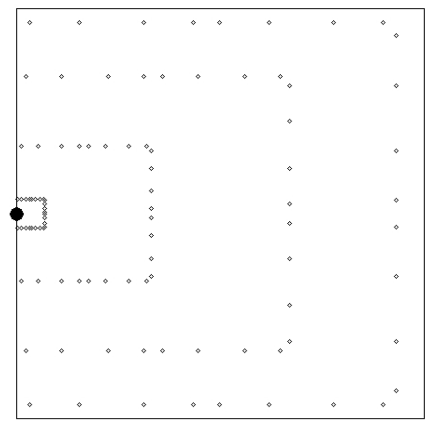

Fig.7 Distribution of integration points after transformation

6.3 Second order singular integrals and nearly singular integrals

When the source point is in the integration element, the integral $\iint_{S_B} \varphi_d{}^{(j)}(\vec{x}_0)\frac{\partial G_0(\vec{x},\vec{x}_0)}{\partial n}ds$ and $\iint_{S_B} \varphi_d{}^{(j)}(\vec{x})\frac{\partial G^{(j)}(\vec{x},\vec{x}_0)}{\partial n}ds$ have second order singularity. When the source point is very close to the integration element, the integral $\iint_{S_B} \varphi_d{}^{(j)}(\vec{x}_0)\frac{\partial G_0(\vec{x},\vec{x}_0)}{\partial n}ds$ and $\iint_{S_B} \varphi_d{}^{(j)}(\vec{x})\frac{\partial G^{(j)}(\vec{x},\vec{x}_0)}{\partial n}ds$ have second order nearly singularity. Evaluating the two integrals respectively would also introduce appreciable errors. However, the singularity of integral $\iint_{S_B} \varphi_d{}^{(j)}(\vec{x}_0)\frac{\partial G_0(\vec{x},\vec{x}_0)}{\partial n}ds$ and $\iint_{S_B} \varphi_d{}^{(j)}(\vec{x})\frac{\partial G^{(j)}(\vec{x},\vec{x}_0)}{\partial n}ds$ in the integral equation (11) can cancel out. The accurate integral results can be obtained by the direct method.

7. Numerical results

To validate the present method, a fixed uniform cylinder under effect of regular waves is considered (see Fig.8). For comparing with the results of Eatock Taylor and Hung (1987), the radius of the cylinder is taken equal to the water depth, i.e. a=d=1.0 m. The incident wave is of 1.0 m amplitude. And all forces are given in Newtons.

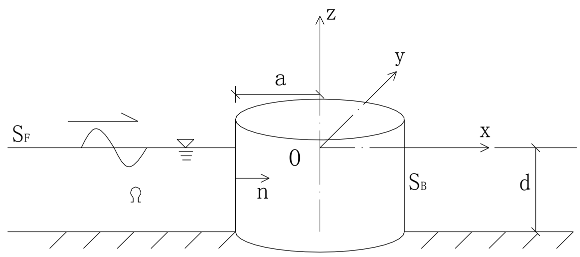

Fig.8 Uniform cylinder under the action of regular waves

Since the uniform cylinder has two planes of symmetry in its geometry, only a quadrant of the wet body surface and free surface (see Fig.9) are meshed, either for the corresponding inner water plane (see Fig.10).

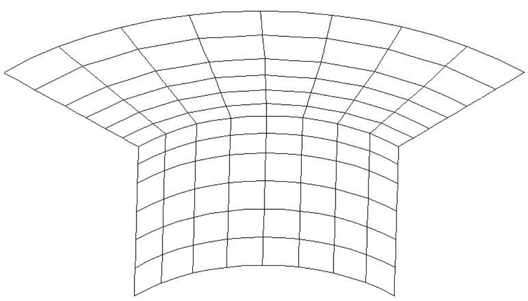

Fig.9 Elements on the body surface and free surface

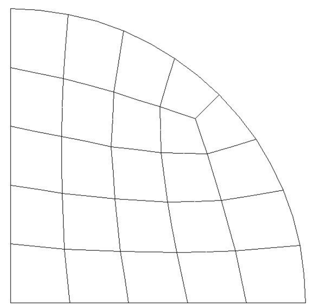

Fig.10 Elements on the inner water plane

7.1 The influence of collocation parameter on numerical results

Because discontinuous elements are used in the present method, it is necessary to examine the influence of collocation parameter β on the accuracy of numerical results. When collocation points on the inner water plane are too close to the body surface, nearly singular integrals would affect the numerical results.

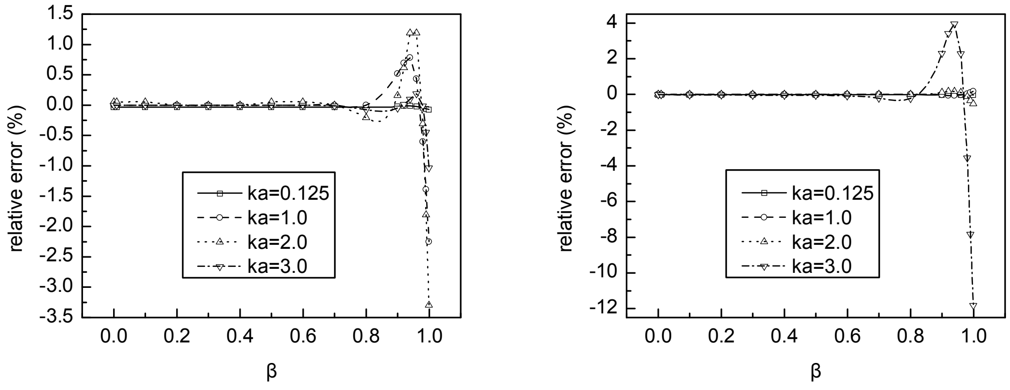

(a) real part (b) imaginary part

Fig.11 Relation between relative errors and collocation parameter for the first order horizontal wave forces

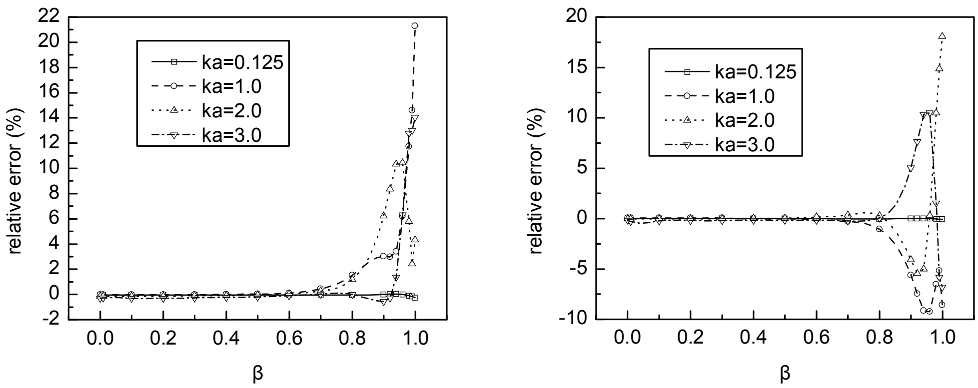

(a) real part (b) imaginary part

Fig.12 Relation between relative errors and collocation parameter for the second order horizontal wave forces (part from second order potential)

Fig.11 shows the relative error between numerical results and analytical solutions (MacCamy and Fuchs, 1954; Eatock Taylor and Hung, 1987) for the first order horizontal wave forces at different β . Fig.12 shows the corresponding comparisons for the second order horizontal wave force between the present numerical results and semi-analytical solutions (Eatock Taylor and Hung, 1987). From the comparisons, we can conclude that collocation parameter can be 0~0.7 in discontinuous elements for most practical engineering problems.

To further validate present numerical results, more results are tabulated (see Table 1 and see Table 2) to compare with analytical and semi-analytical solutions (Eatock Taylor and Hung, 1987). Based on the foregoing discussion, parameter of collocation point is selected as $\beta = 0.5$ in the following examination.

It can be seen that present results are in good agreement with analytical and semi-analytical solutions. Thus analyses of removing irregular frequencies can be carried out trustily.

Table 1 comparison on first order forces

ka	Present results		Analytical solutions	
	Re	Im	Re	Im
0.125	9.834E+01	-7.956E+03	9.837E+01	-7.957E+03
0.25	7.854E+02	-1.590E+04	7.856E+02	-1.590E+04
0.50	5.231E+03	-2.879E+04	5.232E+03	-2.880E+04
0.75	1.057E+04	-3.305E+04	1.057E+04	-3.305E+04
1.00	1.155E+04	-3.090E+04	1.155E+04	-3.090E+04
1.25	8.886E+03	-2.717E+04	8.889E+03	-2.717E+04
1.50	5.008E+03	-2.354E+04	5.009E+03	-2.354E+04
1.75	1.238E+03	-2.016E+04	1.239E+03	-2.017E+04
2.00	-1.940E+03	-1.696E+04	-1.939E+03	-1.696E+04
2.25	-4.403E+03	-1.389E+04	-4.404E+03	-1.390E+04
2.50	-6.166E+03	-1.097E+04	-6.167E+03	-1.097E+04
2.75	-7.289E+03	-8.204E+03	-7.289E+03	-8.207E+03
3.00	-7.847E+03	-5.647E+03	-7.847E+03	-5.650E+03

Table 2 comparison on second order forces (part from second order potential)

ka	Present results		Semi-analytical solutions	
	Re	Im	Re	Im
0.125	3.909E+04	-7.754E+05	3.911E+04	-7.755E+05
0.25	7.142E+04	-3.649E+05	7.144E+04	-3.649E+05
0.50	4.476E+04	-9.991E+04	4.477E+04	-9.992E+04
0.75	1.140E+04	-3.301E+04	1.140E+04	-3.301E+04

1.00	8.940E+03	-1.183E+04	8.937E+03	-1.183E+04
1.25	1.805E+04	-3.040E+03	1.804E+04	-3.038E+03
1.50	2.686E+04	-1.129E+03	2.687E+04	-1.116E+03
1.75	2.889E+04	-5.451E+03	2.888E+04	-5.433E+03
2.00	2.261E+04	-1.531E+04	2.262E+04	-1.531E+04
2.25	1.020E+04	-2.756E+04	1.022E+04	-2.753E+04
2.50	-4.628E+03	-3.681E+04	-4.647E+03	-3.683E+04
2.75	-1.871E+04	-3.787E+04	-1.873E+04	-3.790E+04
3.00	-2.989E+04	-2.807E+04	-2.995E+04	-2.811E+04

7.2 Results of removing irregular frequencies

In the subsequent analyses, the method based on Eq. (11) is called as 'Method A'; the method based on modified integral equations is called as 'Method B'. The distribution of elements is shown in Fig.9 and Fig.10.

7.2.1 First order horizontal wave force

The numerical results for first order horizontal wave force at different wave numbers are compared in Fig.13. In the range of $ka < 3.0$ (see Fig.13 (a)-(c)), Method A and Method B have good agreements, and there are not any irregular frequencies for the first order problem (But we can find that irregular frequencies will produce appreciable errors for the second order problem in this range). For higher frequencies (see Fig.13 (d)-(f)), we will find the irregular frequencies in numerical results by Method A, and Method B can get results free of the irregular frequencies.

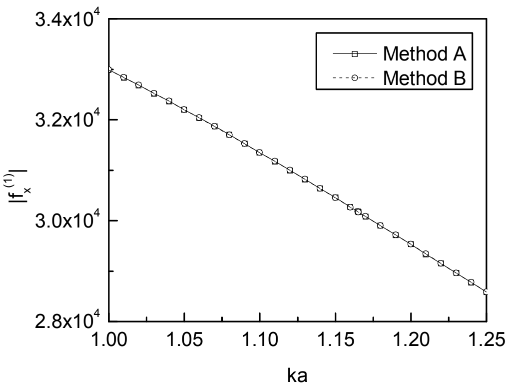

(a)

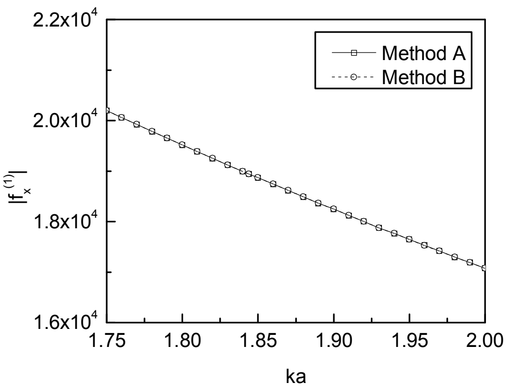

(b)

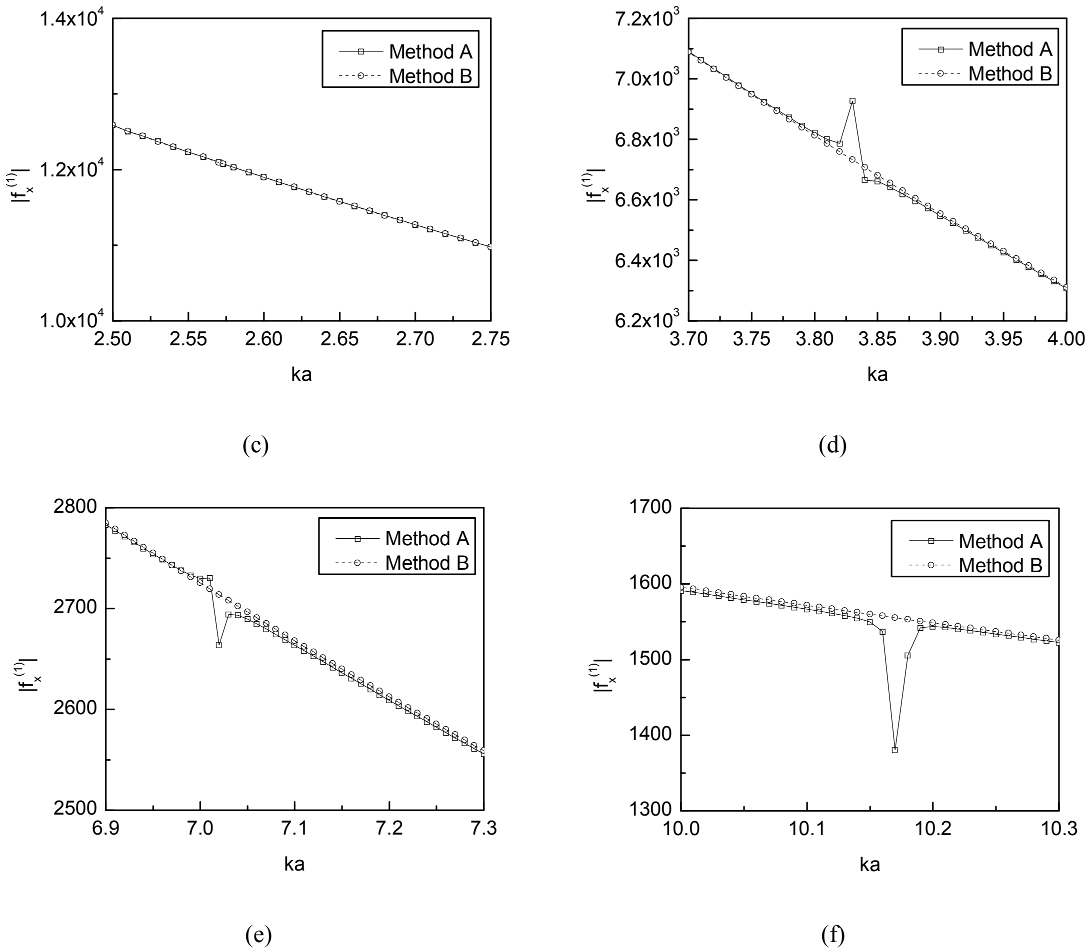

Fig.13 Comparisons for the first order horizontal wave force

7.2.2 Second order horizontal wave force

The numerical results for second order horizontal wave force at different wave numbers are compared in Fig.14. Method A and Method B have good agreements at most part of the computation. But for method A, 'jumps' arise at some frequencies. It is the polluted bands of irregular frequencies. Method B can remove irregular frequencies successfully and get accurate results.

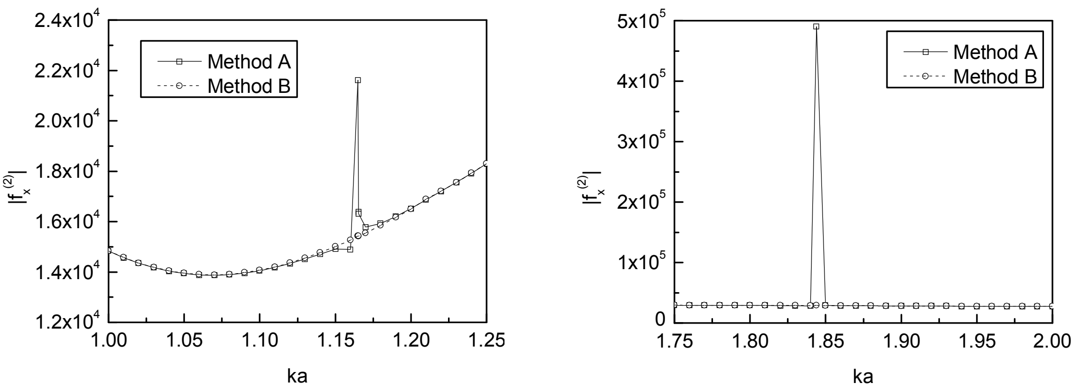

(a) (b)

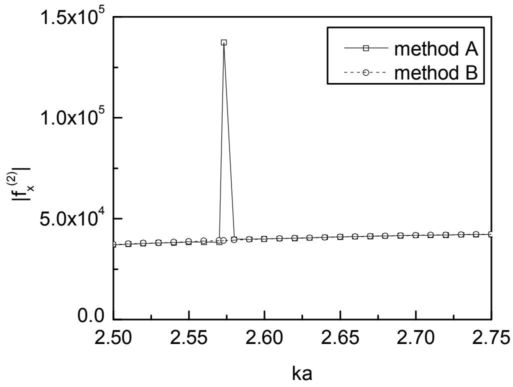

(c)

Fig.14 Comparisons for the second order horizontal wave force (part from second order potential)

The results of the first order and the second order problems also show the importance of removing irregular frequencies for computation, especially for higher order problem. In practical engineering problems, irregular frequencies will more possibly pollute the concerned range in higher order problem.

8. Conclusions

In this paper, continuous higher order boundary elements and partial discontinuous higher order boundary elements are used to discretize the modified integral equations. Numerical examples show that the present method can get high-precise results of wave force for arbitrary bodies without irregular frequencies in both the first order and the second order problems. In practical computation, it is better to select a small value of β (parameter of collocation points) in the range of 0~0.7 to weaken the influence of nearly singularity. At the same time, necessary strategies have to be adopted to deal with the singular and nearly singular integrals.

Acknowledgements

The present work was financially supported by the National Natural Science Foundation of China (Grant No. 10372020) and the Program for Changjiang Scholars and Innovative Research Team in University (Grant No. IRT0420).

References

Chau, F. P., 1989. The second order velocity potential for diffraction of waves by fixed offshore structures. Ph.D. thesis, University of London. (Department of Mechanical Engineering, University College London, Rep. OEG/89/1)

Chau, F. P., Eatock Taylor, R., 1988. Second-order velocity potential for arbitrary bodies in waves. Proc. 3rd Int. Workshop on Water Waves and Floating Bodies, Woods Hole, Mass., pp.15-19.

Duan, W. Y., He, W. Z., 2002. A boundary element method for removing the effects of irregular frequency in solving the hydrodynamic coefficients, J. of hydrodynamics (Ser.A) 17(2), 156-161. (In Chinese)

Eatock Taylor, R., Hung, S. M., 1987. Second order diffraction forces on a vertical cylinder in regular waves. Appl. Ocean Res. 9(1), 19-30.

John, F., 1950. On the motion of floating bodies Ⅱ. Comm. Pure Appl. Math.3, 45-101.

Lamb, H., 1932. Hydrodynamics, Dover, New York.

Lee, C. H., Sclavounos, P. D., 1989. Removing the irregular frequencies from integral equations in wave-body interaction, J. Fluid Mech. 207, 393-418.

Li, H. B., Han, G. M., Mang, H. A., 1985. A new method for evaluating singular integrals in stress analysis of solids by the direct boundary element method, Int. Journal for Numerical Methods in Engineering 21, 2071-2098.

MacCamy, R.C., Fuchs, R. A., 1954.Wave forces on piles: a diffraction theory. Tech. Mem., 69, US Army Coastal Engineering Research Center.

Mei, C. C., 1989. The applied dynamics of ocean surface waves, World Scientific, Singapore.

Molin, B., 1979. Second order diffraction loads upon three-dimensional bodies. Appl. Ocean Res.1, 197-202.

Ogilvie, T. F., Shin, Y. S., 1978. Integral-equation solutions for time-dependent free-surface problems. J. Soc. Nav. Arch. Japan 143, 86-96.

Ohmatsu, S., 1983. A new simple method to eliminate the irregular frequencies in the theory water wave radiation problem, Ship Res. Inst., Japan (Papers, No.70).

Sun, L., Teng, B., Ning, D.Z. A self-adaptive Gauss integral method for evaluation of nearly singular integrals (Accepted by Journal of Dalian University of Technology). (In Chinese)

Teng, B., Eatock Taylor, R., 1995. New higher-order boundary element methods for wave diffraction/radiation. Appl. Ocean Res.17, 71–77.

Teng, B., Kato, S., 1999. A method for second-order diffraction potential from an axisymmetric body. Ocean Engineering 26, 1359–1387.

Teng, B., Li, Y. C., 1996. A unique solvable higher order BEM for wave diffraction and radiation. China Ocean Engineering 10(3), 333-342.

Ursell, F., 1981. Irregular frequencies and the motion of floating bodies. J. Fluid Mech. 105, 143-156.